

## The temperature effect on the production of liquid and solid fuel via wood pellet torrefaction

Cheolwoo Park\*, Eun-Suk Jang<sup>\*,†</sup>, and Young-Min Kim<sup>\*\*,†</sup>

\*Plant Process Development Center, Institute for Advanced Engineering, Yongin 17180, Korea

\*\*Department of Environmental Engineering, Daegu University, Gyeongsan 38453, Korea

(Received 11 July 2022 • Revised 12 September 2022 • Accepted 29 September 2022)

**Abstract**—The effects of temperature on the product quality of wood pellet torrefaction were examined by performing experiments, proximate analysis, ultimate analysis, heating value measurement, thermogravimetric analysis, and moisture absorption of torrefied wood pellets at 250, 300, 350, and 400 °C. The liquids produced during torrefaction and high-temperature pyrolysis of torrefied wood pellet at 800 °C were also analyzed. By increasing the torrefaction temperature to 400 °C, the yield of the solid was decreased to 30.32%, with an increase in gas (17.53%) and liquid (52.16%) yield caused by the partial elimination and decomposition of hemicellulose, cellulose, and lignin of wood pellet. The higher heating value of wood pellets was increased from 4,670 kcal/kg for raw wood pellets to 7,480 kcal/kg for torrefied wood pellets at 400 °C with the carbon concentration during torrefaction. Although the carbon density and heating value of the wood pellets were improved, overall energy recovery efficiency was decreased because of the decrease in solid yield by torrefaction. Thermogravimetric analysis results suggested that thermally stable wood pellet formation is formed by the elimination and structural changes to hemicellulose, cellulose, and lignin. The hydrophobicity of wood pellets was increased by torrefaction leading to the elimination of the hydrophilic functional groups of wood pellets. The moisture absorption of wood pellets (14.95%) was also decreased to 5.09% for torrefied wood pellets. Low-temperature torrefaction between 250 and 300 °C produced the typical pyrolyzates of hemicellulose and cellulose, such as furans and acids. The amount of lignin pyrolyzates, such as guaiacol, eugenol, and other phenolics, was increased by applying high-temperature torrefaction at 400 °C. The solid fuel produced by the high-temperature torrefaction of wood pellets also provided a potential decreasing tar content during gasification, indicating the improved process efficiency of torrefied wood pellets.

Keywords: Wood Pellet, Torrefaction, Bio-fuel, Gasification, Tar Reduction

### INTRODUCTION

Global efforts to minimize climate change by reducing greenhouse emissions have been a major focus in recent decades. Many countries have announced new policies to reduce carbon emissions and develop eco-friendly energy sources to replace fossil fuels, but the proportion of fossil fuels is still high [1,2]. The importance of biomass has been emphasized to mitigate the depletion of fossil fuels and excessive carbon emission because of its abundance and carbon neutrality. Biomass can be used as a simple heat source and converted to gas, liquid, and solid fuel via thermal treatment technologies, such as torrefaction, pyrolysis, and gasification. On the other hand, the fuel properties of biomass, such as heating value, moisture content, and water absorption, are lower than that of coal, and additional pretreatment of biomass is required to use biomass as a fuel.

Biomass torrefaction is a thermal treatment method that increases the fuel property of biomass fuel by applying low-temperature heat between 200 and 300 °C under an inert atmosphere, leading to the partial decomposition of hydrophilic functional groups, such as

hydroxyl and methoxy groups. This can lead to improved biomass hydrophobicity and heat density [3]. The torrefaction temperature is the most important parameter. Many researchers have reported the effect of the torrefaction temperature on solid product quality. The product quality of biomass torrefaction is differentiated by the composition of the biomass components, hemicellulose, cellulose, and lignin, and their decomposition temperature. Many researchers have reported the effects of torrefaction on the quality improvement of the product quality.

Lee et al. [4] reported that the main functional groups of hemicellulose and cellulose in biomass could be decomposed easily during the torrefaction of sugarcane bagasse, leading to a large change in the physical properties of biomass. Niu et al. [5] indicated that the crystallinity of cellulose was improved at temperatures higher than 250 °C, leading to increased heat transfer of torrefied biomass. Eseyin et al. [6] compared the energy recovery of torrefied biomass from empty fruit bunches, mesocarp fiber, and kernel shells and reported the improved fuel property of torrefied biomass. Meng et al. [7] reported that the heating value of biomass was also increased by the torrefaction of biomass, indicating the reaction mechanism.

The above researchers suggest that the quality of the emitted gas and oil products is differentiated by torrefaction, and temperature is the most critical factor in fuel upgrading, but the oil quality produced from biomass torrefaction was not investigated. In addition,

<sup>†</sup>To whom correspondence should be addressed.

E-mail: janges95@iae.re.kr, ymk@daegu.ac.kr

Copyright by The Korean Institute of Chemical Engineers.

high-temperature torrefaction is necessary for using a torrefied solid product as a fuel or fuel source. On the other hand, the studies of the effect of the torrefaction temperature on the use of the final product have not been systematic.

Therefore, this study examined the effects of biomass torrefaction on producing high-quality solid fuel and on oil quality formed during biomass torrefaction and the advantage of high-temperature torrefied fuel via various experiments, such as water absorption resistance and tar formation during the gasification of torrefied biomass.

## EXPERIMENTS

### 1. Wood Pellet Torrefaction

The feeding sample was used as a biomass sample and torrefied using a semi-batch type reactor, as shown in Fig. 1. The sample was acquired from the commercial wood pellet (WP) fuel from a pelletized forestry byproduct with a diameter of 6 mm and containing 6.74% moisture, 76.84% volatile matter (VM), 15.76% fixed carbon (FC), and 0.66% ash. For torrefaction, 1 kg of biomass in a reactor was heated to different temperatures, 250, 300, 350, and 400 °C under 150 mL/min of nitrogen gas. The product vapor emitted from the reactor during torrefaction was condensed at 5 °C and collected in a liquid collection flask. After torrefaction, the torrefied WP (TWP) that remained in the reactor was collected. The yields of liquid and torrefied biomass were calculated by measuring the collected weight of liquid and torrefied char, as shown in the equations below.

$$y_s = \frac{m_s}{m_i} \times 100 (\%) \quad (1)$$

$$y_l = \frac{m_l}{m_i} \times 100 (\%) \quad (2)$$

$$y_g = 100 - y_s - y_l (\%) \quad (3)$$

Here,  $y_s$ ,  $y_l$ , and  $y_g$  are the yield of solid, liquid, and gas product, respectively, and  $m_p$ ,  $m_s$ , and  $m_l$  are the weight of initial biomass, torrefied biomass, and collected liquid, respectively. The gas yield was obtained by subtracting the summed yield of liquid and torrefied biomass from the feeding biomass.

### 2. Physico-chemical Properties of Torrefied Biomass

Various experiments, proximate analysis, ultimate analysis, and heating value measurement were performed to determine the fuel property change of torrefied biomass. Proximate analysis was performed using standard methods (ASTM D3172-13). Ultimate analysis involved using an elemental analyzer (EA1112, Thermo Fisher Scientific), and the heating value was measured using a bomb calorimeter (Isoperibol, Parr). Thermogravimetric analysis (TGA, TG-55, TA Instrument) was performed to check the thermal property of the torrefied biomass by heating 5 mg each of biomass and torrefied biomass from 40 °C to 900 °C at 5 °C/min under 60 mL/min of nitrogen gas. The energy recovery efficiency (ERE) of the torrefaction process was calculated using the following equation:

$$ERE = \frac{CV_{tb}}{CV_{fb}} \times y_{tb} \quad (4)$$

where  $CV_{tb}$  and  $CV_{fb}$  are the calorific values of torrefied biomass and feeding biomass.  $y_{tb}$  is the yield of torrefied biomass.

### 3. Hygroscopicity Test

Moisture absorption is important in the transport and storage of solid fuels. The volume of raw WP (RWP) can be increased easily due to their easy water absorption, which can cause low moldability and easy decay, decreasing the fuel quality [10]. A hygroscopicity test was performed based on the standard method (KS F2205, [10]) to check the advantage of torrefied biomass on its

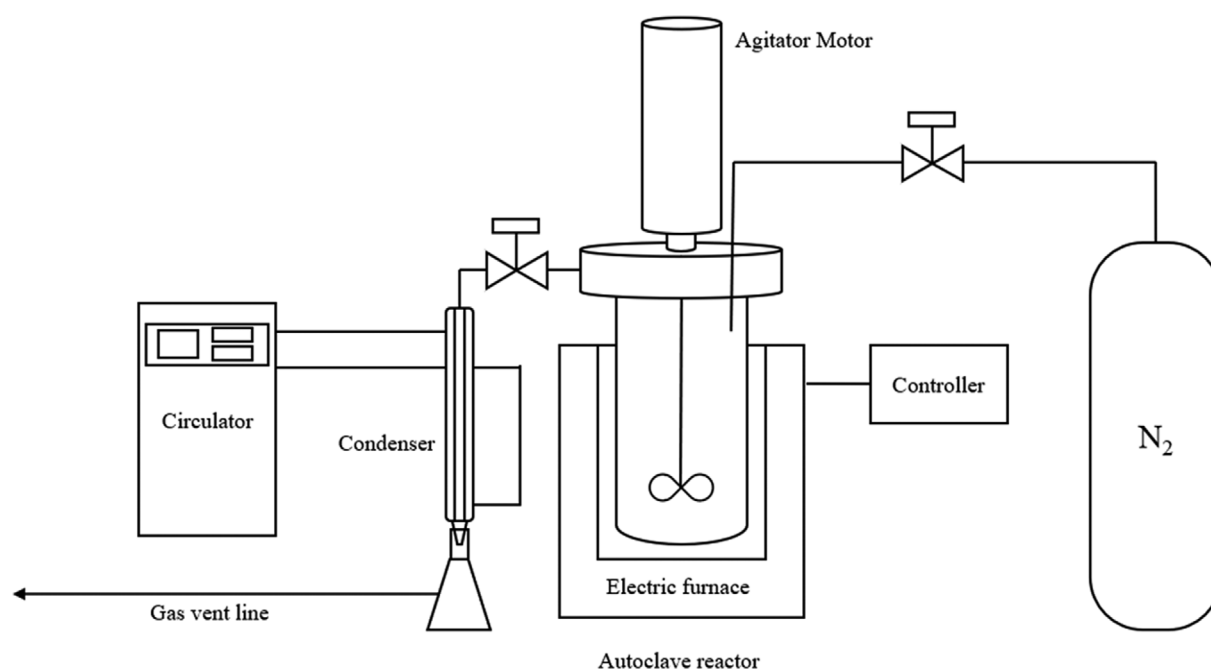


Fig. 1. Schematic diagram of torrefaction reactor system.

transport and storage. Briefly, 2 g of torrefied biomass was dried at  $105\pm 2^\circ\text{C}$  for 48 hours and put in a constant temperature and humidity tank (HB-105SG, Han Baek Scientific Co.) at  $40\pm 1^\circ\text{C}$  with a relative humidity of  $75\pm 1\%$  for 24 hours. The weight change in the torrefied biomass after moisture absorption was measured, and final hygroscopicity ( $M$ , %) was calculated using the following:

$$M = \frac{W_{\text{after}} - W_{\text{before}}}{W_{\text{before}}} \times 100 \quad (\%) \quad (5)$$

where  $W_{\text{before}}$  and  $W_{\text{after}}$  are the weight of torrefied biomass before and after water absorption.

To determine the relationship between the surface functional group of torrefied biomass and hygroscopicity, Fourier-transform infrared spectroscopy (FT-IR, Nicolet iS50, Thermo Scientific) of torrefied biomass was performed between  $4,000$  and  $500\text{ cm}^{-1}$ .

#### 4. Liquid Product of Biomass Torrefaction

The chemical distribution of liquid product formed during biomass torrefaction was analyzed using gas chromatography/mass spectrometry (GC/MS, 7890A/5975C, Agilent Technology). Briefly,  $1\ \mu\text{l}$  of liquid was injected into the GC inlet ( $320^\circ\text{C}$ , split ratio 100/1) and separated in a capillary column (UA-5, 30 m length  $\times$  0.25 mm inner diameter  $\times$  0.25  $\mu\text{m}$  film thickness) installed in a programmed GC oven from  $40^\circ\text{C}$  to  $320^\circ\text{C}$  at  $20^\circ\text{C}/\text{min}$ . The separated chemicals were identified by comparing the mass spectrum of each peak on the total ion chromatogram (TIC) with that in libraries (Nist 08<sup>th</sup>, F-Search library). The amount of each chemical generated from the biomass torrefaction at different temperatures was evaluated by comparing the absolute peak area of each chemical monitored in TIC.

#### 5. High-temperature Pyrolysis

High-temperature pyrolysis-GC/MS analysis of torrefied biomass was performed to determine the potential tar formation when the torrefied biomass was applied as a feedstock to the gasification process. For this, 0.3 mg of torrefied biomass was pyrolyzed in a furnace-type pyrolyzer (PY-3030D, Frontier Laboratories) at  $800^\circ\text{C}$ , and product vapor was analyzed by the GC/MS under the same analysis condition applied to liquid product analysis during torrefaction.

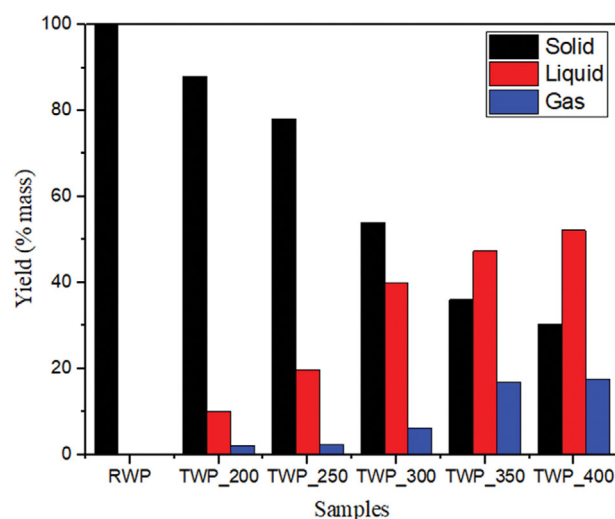


Fig. 2. Product yields from WP torrefaction experiments.

## RESULTS AND DISCUSSION

### 1. Biomass Torrefaction

Fig. 2 presents the yields of gas, liquid, and solid product obtained from the torrefaction of WPs at different temperatures. The solid yield decreased with increasing torrefaction temperature. The gas and liquid yields also increased with increasing torrefaction temperature. Interestingly, an increase in torrefaction temperature from  $250^\circ\text{C}$  to  $300^\circ\text{C}$  led to a significant change in product yield because of the initial decomposition of biomass components, hemicellulose, cellulose, and lignin. Kim et al. [13] suggested that the decomposition of hemicellulose and lignin is initiated at  $200^\circ\text{C}$  and continues up to  $300^\circ\text{C}$  and  $600^\circ\text{C}$ , respectively. Cellulose is decomposed sharply between  $300^\circ\text{C}$  and  $400^\circ\text{C}$ . Lee et al. [4] indicated that hemicellulose is decomposed mainly between  $245^\circ\text{C}$  and  $290^\circ\text{C}$ , suggesting that the large change in gas, liquid, and solid yield caused by increasing torrefaction temperature from  $250^\circ\text{C}$  to  $300^\circ\text{C}$  was due to the decomposition of hemicellulose in WPs. Kim et al. [12]

Table 1. Proximate, elemental, and calorific value analyses of the WP samples

Samples	Raw WP	TWP_250	TWP_300	TWP_350	TWP_400
Proximate analysis (db, wt%)					
Moisture%	6.74	4.67	1.21	-	-
Volatiles%	76.84	67.23	49.19	31.06	39.42
Fixed carbon%	15.76	26.83	47.94	67.30	58.89
Ash%	0.66	1.26	1.66	1.64	1.70
Elemental analysis (daf, wt%)					
Carbon%	49.39	53.27	70.74	75.59	82.51
Hydrogen%	6.05	5.90	4.90	4.42	3.38
Nitrogen%	-	0.21	0.26	-	0.15
Oxygen%	43.07	30.96	17.00	17.18	9.20
Sulfur%	-	-	-	-	-
Calorific value (kcal/kg)					
Higher heating value (HHV)	4,670	5,660	6,590	7,020	7,480

indicated that torrefaction between 200 and 300 °C eliminates moisture, volatiles, and hemicellulose with a partial structural change in cellulose and lignin, leading to superior feedstock properties for the post-pyrolysis process. Although the gas yield was increased with increasing liquid yield, it was lower than 10% at temperatures lower than 350 °C, suggesting that primary decomposition and the abstraction of functional groups from biomass components is the main reaction of low-temperature biomass torrefaction. The gas yield was increased from 350 °C, suggesting the secondary cracking of pyrolyzates, accompanied mainly under pyrolysis conditions higher than 600 °C [1], was activated under this high-temperature torrefaction condition.

## 2. Fuel Properties of Torrefied Wood Pellet

Table 1 lists the proximate, ultimate, and heating value analysis results of TWPs. By increasing the torrefaction temperature, fixed carbon was increased from 15.76% (Raw WP) to 67.30% (TWP\_350), with a concomitant decrease in volatiles from 76.84% to 31.06% due to the elimination of thermally weak volatiles and the concentration of thermally stable fixed carbon during torrefaction [13]. The ultimate analysis results also revealed the increase in carbon content up to 75.79% with decreasing oxygen content down to 17.18% by increasing the torrefaction temperature to 400 °C, leading to an increase in heating value to 7,480 kcal/kg. Other studies also reported a similar tendency for the change in fuel property of wood biomass by the change in torrefaction temperature [3,14,15].

The van Krevelen plot of TWPs (Fig. 3) indicated that hydrogen to carbon (H/C) and oxygen to carbon (O/C) ratios was decreased together by increasing the torrefaction temperature. Hydrophilic functional groups, such as hydroxyl and carboxylic groups, are extracted easily at torrefaction temperature and generate hydrophilic liquid products with large amounts of water and carbon dioxide formation [4,16]. In the present results, TWP-300, TWP-350, and TWP-400 had similar H/C and O/C ratios with bituminous residue due to the effective high-temperature torrefaction, suggesting the feasibility of these TWPs as a potential fuel. On the other hand, the ERE of torrefaction was also decreased with in-

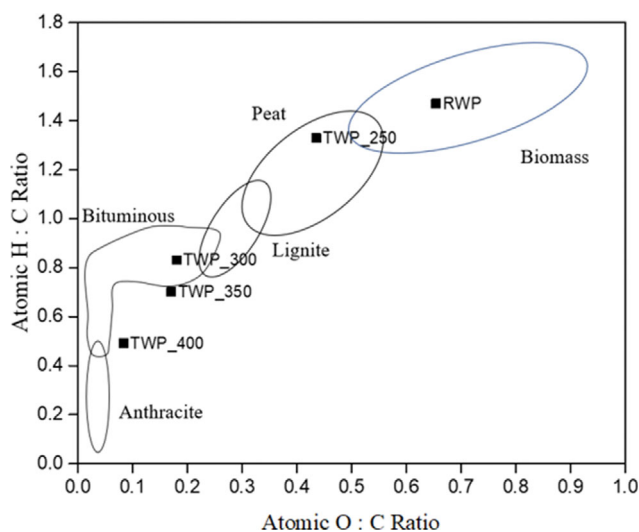


Fig. 3. Van Klevelen plot of the RWP and TWPs.

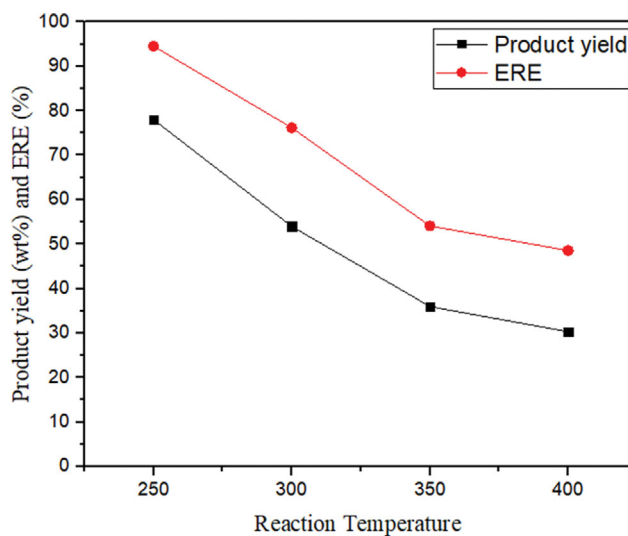
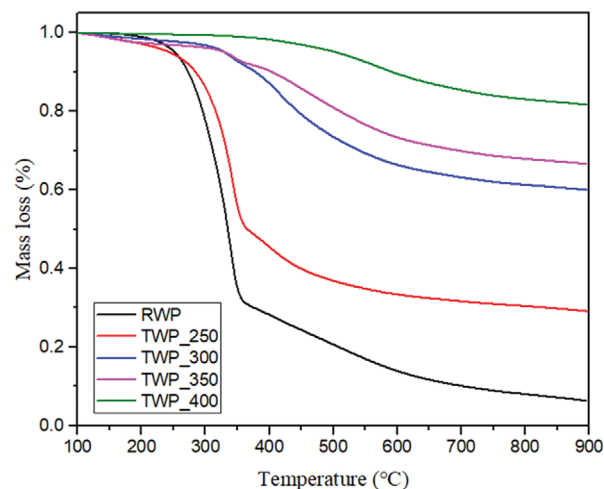
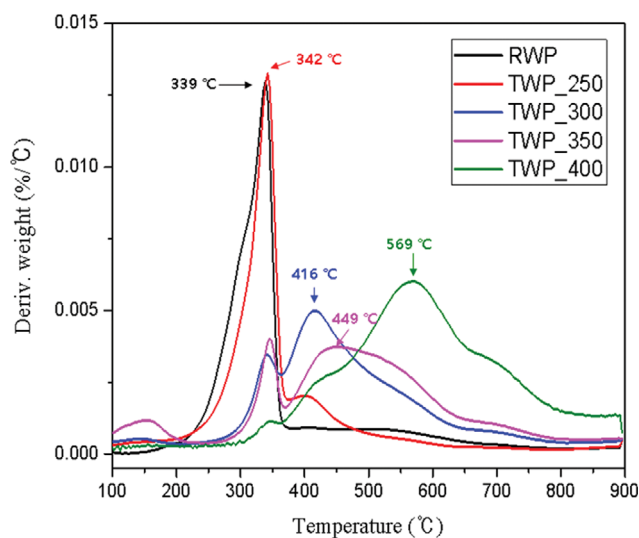


Fig. 4. Torrefaction temperature effect on product yield and ERE.



(a) TG



(b) DTG

Fig. 5. TG and DTG curves of RWP and TWPs.

creasing reaction temperature and decreasing TWP yield (Fig. 4). This suggests that it is necessary to determine the optimal torrefaction operating conditions, such as calorific value and yield change of solid products, for applications to energy recovery and process operation stability assurance.

### 3. TGA

Fig. 5 presents the TGA and derivative TG (DTG) curves of RWP and TWPs. The DTG curve of RWP shows that the typical DTG curve of woody biomass [17,18] consists of the overlapped decomposition of hemicellulose, cellulose, and lignin [3,19]. The DTG peak height of the TWP at 250 °C (TWP\_250) is lower than that of the RWP, confirming the partial elimination of hemicellulose by the torrefaction of RWP at 250 °C. Furthermore, the DTG peak intensity of TWP\_250 is increased at temperatures higher than 350 °C, suggesting that thermally stable biochar is generated during the torrefaction of RWP at 250 °C.

In the case of TWP\_300, the decomposition peak of cellulose between 300 °C and 350 °C [20,21] also decreased with increasing DTG peak height at temperatures higher than 400 °C. This also suggests that a large amount of thermally more stable biochar is generated during the torrefaction at 300 °C. Although a large amount of thermally stable biochar was formed with the elimination of hemicellulose and cellulose during torrefaction at 300 °C, it is difficult to understand the char formation via the decomposition of hemicellulose and cellulose because the char yields of hemicellulose and cellulose are smaller than that of lignin during their TG analysis [6]. Therefore, the formation of thermally stable biochar in TWP\_300 is caused mainly by the partial decomposition of lignin and the formation of thermally stable biochar with an increased carbon density. TWP\_350 had a higher DTG peak height than TWP\_300 at a higher temperature than 400 °C, and the DTG peak temperature of TWP\_350 became higher than that of TWP\_300, suggesting the thermal stability of TWP is further increased by applying the higher torrefaction temperature.

### 4. Hygroscopicity Test

Moisture absorption of WP, 14.95%, decreased primarily to 9.48% after the torrefaction at 250 °C and further decreased to 5.09% by

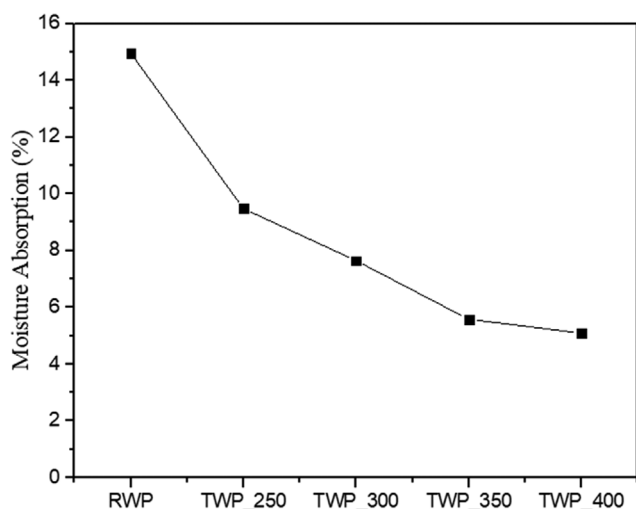


Fig. 6. Water uptake of RWP and TWPs after hygroscopicity test.

increasing the torrefaction temperature up to 400 °C, as shown in Fig. 6. The decrease in moisture absorption can be explained by the surface property of TWP. As shown in Fig. 7, the peak intensity of the hydrophilic group at 3,280  $\text{cm}^{-1}$  (-OH) and 2,918  $\text{cm}^{-1}$  (C-H) on the FT-IR spectrum of the TWPs decreased with increasing torrefaction temperature. Peak intensity at 1,020-1,040  $\text{cm}^{-1}$ , indicated C=C, C-O, and C-O-C of hemicellulose, cellulose, and lignin [3]. Peak intensity at 1,700-1,740  $\text{cm}^{-1}$  (carbonyl and carboxyl group [22,23]) also decreased with increasing torrefaction temperature due to the depolymerization of cellulose and hemicellulose [24]. The above results suggest that the hydrophilic functional group of WPs is eliminated during the high-temperature torrefaction, and the surface hydrophobicity of TWP is improved, leading to decreased moisture absorption.

### 5. Liquid Product of Wood Pellet Torrefaction

Fig. 8 shows chromatograms of liquids generated during the torrefaction at different temperatures obtained from GC/MS analysis. Various kinds of chemicals were emitted during the torrefaction of WPs. Typical pyrolysis products of hemicellulose (acetic acid and furfural) and lignin (guaiacol) were generated during torrefaction at 250 °C. During the WP torrefaction at 300 °C, the peak intensity for lignin pyrolyzates, such as guaiacol, creosol, and ethylguaiacol, increased in the presence of levoglucosan, the typical pyrolyzate of cellulose [25]. The peak intensity for lignin pyrolyzates was increased further by applying higher temperature torrefaction, suggesting that the main change in TWP property during high-temperature torrefaction is related largely to the decomposition of lignin.

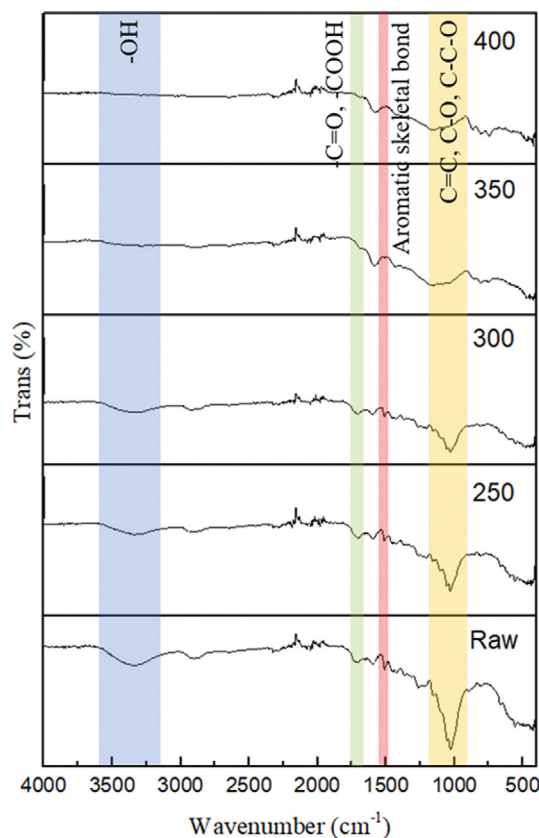
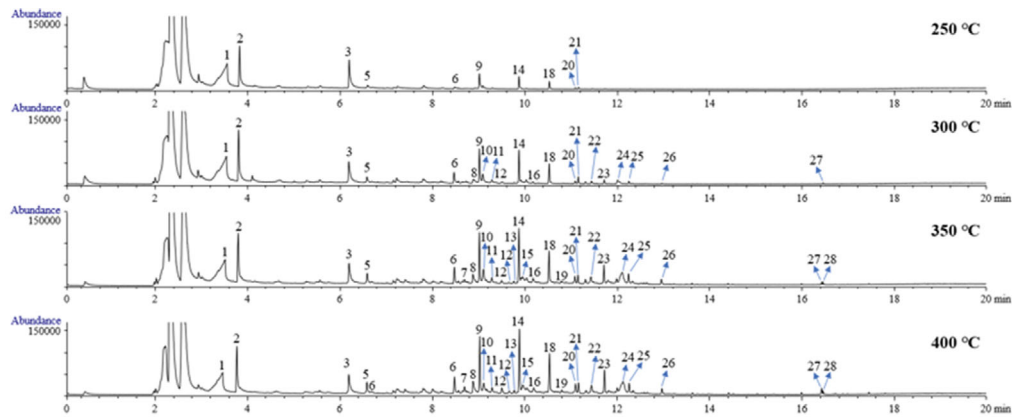
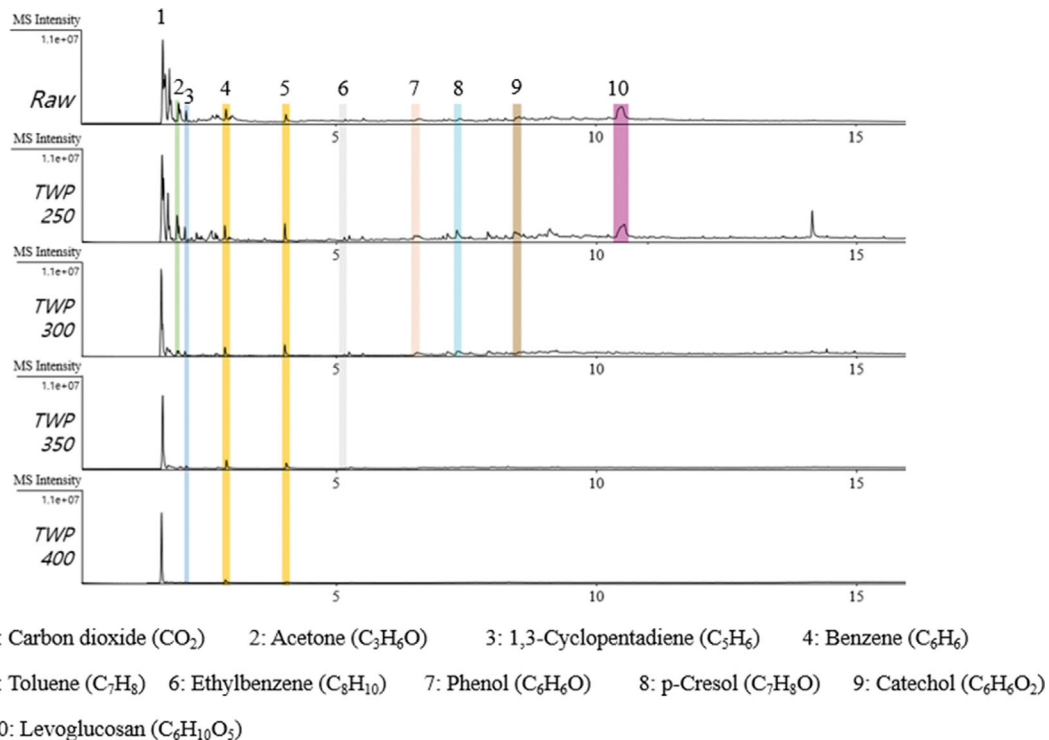


Fig. 7. FT-IR spectrum of RWP and TWPs.



- 1: Acetic acid (C<sub>2</sub>H<sub>4</sub>O<sub>2</sub>)      2: Hydroxypropanone (C<sub>3</sub>H<sub>6</sub>O<sub>2</sub>)      3: 2-Furfural (C<sub>5</sub>H<sub>4</sub>O<sub>2</sub>)      4: 2-Furanmethanol (C<sub>5</sub>H<sub>6</sub>O<sub>2</sub>)  
 5: 2,3-Butanedione (C<sub>4</sub>H<sub>6</sub>O<sub>2</sub>)      6: 2-Hydroxy-1-methylcyclopenten-3-one (C<sub>6</sub>H<sub>8</sub>O<sub>2</sub>)      7: m-Cresol (C<sub>7</sub>H<sub>8</sub>O)      8: p-Cresol (C<sub>7</sub>H<sub>8</sub>O)  
 9: Guaiacol (C<sub>7</sub>H<sub>8</sub>O<sub>2</sub>)      10: Unknown      11: 2-Hydroxy-3,4-dimethyl-2-cyclopenten-1-one (C<sub>7</sub>H<sub>10</sub>O<sub>2</sub>)      12: Dimethylphenols (C<sub>8</sub>H<sub>10</sub>O<sub>2</sub>)  
 13: 2-Methoxy-3-methylphenol (C<sub>8</sub>H<sub>10</sub>O<sub>2</sub>)      14: Creosol (C<sub>8</sub>H<sub>10</sub>O<sub>2</sub>)      15: Ethoxyphenol (C<sub>8</sub>H<sub>10</sub>O<sub>2</sub>)      16: 5-Hydroxymethylfurfural (C<sub>6</sub>H<sub>6</sub>O<sub>3</sub>)  
 17: Methylcatechol (C<sub>7</sub>H<sub>8</sub>O<sub>2</sub>)      19: Vinylguaiacol (C<sub>9</sub>H<sub>10</sub>O<sub>2</sub>)      20: Eugenol (C<sub>10</sub>H<sub>12</sub>O<sub>2</sub>)      21: Propylguaiacol (C<sub>10</sub>H<sub>14</sub>O<sub>2</sub>)  
 22: Propenylguaiacol (C<sub>10</sub>H<sub>12</sub>O<sub>2</sub>)      23: Isoeugenol (C<sub>10</sub>H<sub>12</sub>O<sub>2</sub>)      24: Levoglucosan (C<sub>6</sub>H<sub>10</sub>O<sub>5</sub>)?      25: 4-Hydroxy-3-methoxyphenyl acetone (C<sub>10</sub>H<sub>12</sub>O<sub>3</sub>)  
 26: Homovanillic acid (C<sub>9</sub>H<sub>10</sub>O<sub>4</sub>)      26: Homovanillic acid (C<sub>9</sub>H<sub>10</sub>O<sub>4</sub>)      27: Unknown      28: Unknown

Fig. 8. Chromatogram for the liquid product emitted from the WPs during this torrefaction.



- 1: Carbon dioxide (CO<sub>2</sub>)      2: Acetone (C<sub>3</sub>H<sub>6</sub>O)      3: 1,3-Cyclopentadiene (C<sub>5</sub>H<sub>6</sub>)      4: Benzene (C<sub>6</sub>H<sub>6</sub>)  
 5: Toluene (C<sub>7</sub>H<sub>8</sub>)      6: Ethylbenzene (C<sub>8</sub>H<sub>10</sub>)      7: Phenol (C<sub>6</sub>H<sub>6</sub>O)      8: p-Cresol (C<sub>7</sub>H<sub>8</sub>O)      9: Catechol (C<sub>6</sub>H<sub>6</sub>O<sub>2</sub>)  
 10: Levoglucosan (C<sub>6</sub>H<sub>10</sub>O<sub>5</sub>)

Fig. 9. Pyrograms of RWP and TWPs at 800 °C.

## 6. High-temperature Pyrolysis

During the gasification of torrefied biomass, tar formation is considered the limitation, decreasing the overall process efficiency [26], and high-temperature pyrolysis can be an indicator of tar for-

mation in biomass gasification. As shown in Fig. 9, Py-GC/MS analysis of TWPs at 800 °C revealed different pyrograms depending on the torrefaction temperature. Although the pyrogram of TWP<sub>250</sub> was not largely different from that of RWP, that of



TWP\_300 had smaller peak intensities for potential tar products of gasification, such as benzene, toluene, ethylbenzene, and other phenols. TWP\_350 produced small amounts of benzene and toluene. This suggests that the TWP produced at high temperatures (TWP\_400) can provide the highest benefits as a potential fuel, providing a higher heating value, which is an advantage in its transport and storage because of its low hygroscopicity and low tar formation during gasification.

### CONCLUSION

WPs were torrefied at different temperatures from 250 °C to 400 °C. By increasing the torrefaction temperature, the yield of solid decreased with increasing gas and liquid yield. The fuel properties, carbon content, hygroscopicity, and high heating value of TWPs were also improved by applying high-temperature torrefaction. On the other hand, the ERE of torrefaction decreased gradually with increasing torrefaction temperature because of the decrease in TWP yield, suggesting the desirable consideration of torrefaction depending on the target application of torrefied biomass. TGA of torrefied biomass suggested that the improvement in the TWP quality is based on biomass char formation and the elimination of hemicellulose and cellulose. Various kinds of liquid products were produced during the torrefaction of WPs, indicating the potential use of liquid products formed for WP torrefaction. Torrefied biomass formed at high temperature also produced a smaller amount of tar during high-temperature Py-GC/MS analysis, confirming the high feasibility of the TWP as a feedstock for additional gasification. Overall, the obtained results suggest that torrefaction has versatility in pretreatment process for biomass, which can improve fuel properties, chemical production, and tar reduction.

### ACKNOWLEDGEMENTS

This work was supported by Korea Institute of Planning and Evaluation for Technology in Food, Agriculture and Forestry (IPET) and Korea Smart Farm R&D Foundation (KosFarm) through Smart Farm Innovation Technology Development Program, funded by Ministry of Agriculture, Food and Rural Affairs (MAFRA) and Ministry of Science and ICT (MSIT), Rural Development Administration (RDA) (421037031HD020), and this work was supported by the Korea Ministry of Environment as Waste to Energy-Recycling Human Resource Development Project (YL-WE-22-001).

### REFERENCES

- IEA (2021), *World Energy Outlook 2021*, IEA, Paris <https://www.iea.org/reports/world-energy-outlook-2021>.
- Y. H. Oh, I. Y. Eom, J. C. Joo, J. H. Yu, B. K. Song, S. H. Lee, S. H. Hong and S. J. Park, *Korean J. Chem. Eng.*, **32**, 1945 (2015).
- W. H. Chen, J. Peng and X. T. Bi, *Renew. Sust. Energ. Rev.*, **44**, 847 (2015).
- C. G. Lee, M. J. Kim and C. D. Eom, *BioResources*, **17**(1), 411 (2022).
- Y. Niu, Y. Lv, Y. Lei, S. Liu, Y. Liang, D. Wang and S. Hui, *Renew. Sust. Energ. Rev.*, **115**, 109395 (2019).
- A. E. Eseyin, P. H. Steele, C. U. Pittman Jr., K. I. Ekpenyong and B. Soni, *Biofuels*, **7**(1), 20 (2016).
- J. Meng, J. Park, D. Tilotta and S. Park, *Bioresour. Technol.*, **111**, 439 (2012).
- S. U. Lee, K. Jung, G. W. Park, C. Seo, Y. K. Hong, W. H. Hong and H. N. Chang, *Korean J. Chem. Eng.*, **29**, 831 (2012).
- L. Kumar, A. A. Koukoulas, S. Mani and J. Satyavolu, *Energy Fuels*, **31**(1), 37 (2017).
- J. S. Jeong, G. M. Kim, H. J. Jeong, G. B. Kim and C. H. Jeon, *Trans. Korean Hydrogen New Energy Soc.*, **30**(1), 49 (2019).
- T. U. Han, Y. M. Kim, C. Watanabe, N. Teramae, Y. K. Park, S. Kim and Y. Lee, *J. Ind. Eng. Chem.*, **32**, 345 (2015).
- Y. M. Kim, J. Jae, B. S. Kim, Y. Hong, S. C. Jung and Y. K. Park, *Energy Convers. Manag.*, **149**, 966 (2017).
- A. Anca-Couce, *Prog. Energy Combust. Sci.*, **53**, 41 (2016).
- J. Wang, B. Shen, D. Kang, P. Yuan and C. Wu, *Chem. Eng. Sci.*, **195**, 767 (2019).
- D. Mohan, C. U. Pittman Jr. and P. H. Steele, *Energy Fuels*, **20**(3), 848 (2006).
- P. K. Dikshit, H. B. Jun and B. S. Kim, *Korean J. Chem. Eng.*, **37**(3), 387 (2020).
- Y. H. Park, J. Kim, S. S. Kim and Y. K. Park, *Bioresour. Technol.*, **100**, 400 (2009).
- L. Zhu and Z. Zhong, *Korean J. Chem. Eng.*, **37**, 1660 (2020).
- P. R. Patwardhan, R. C. Brown and B. H. Shanks, *ChemSusChem*, **4**, 1629 (2011).
- H. J. Park, J. I. Dong, J. S. Kim, J. K. Jeon, S. S. Kim, J. Kim, B. Song, J. Park, K. J. Lee and Y. K. Park, *Fuel Process. Technol.*, **90**, 186 (2009).
- Y. K. Park, M. L. Yoo, H. W. Lee, S. S. Park, S. C. Kim, S. H. Park and S. C. Jung, *Renew. Energy*, **42**, 125 (2012).
- D. A. Granados, R. A. Ruiz, L. Y. Vega and F. Chejne, *Energy*, **139**, 818 (2017).
- J. Park, J. Meng, K. H. Lim, O. J. Rojas and S. Park, *J. Anal. Appl. Pyrolysis*, **100**, 199 (2013).
- K. Manatura, *Case Stud. Therm. Eng.*, **19**, 100623 (2020).
- C. R. Lee, J. S. Yoon, Y. W. Suh, J. W. Choi, J. M. Ha, D. J. Suh and Y. K. Park, *Catal. Commun.*, **17**, 54 (2012).
- H. J. Park, S. H. Park, J. M. Sohn, J. Park, J. K. Keon, S. S. Kim and Y. K. Park, *Bioresour. Technol.*, **101**, S101 (2010).